Biochemistry

 Volume 37, Number 28 July 14, 1998

Accelerated Publications

Direct Spectroscopic and Kinetic Evidence for the Involvement of a Peroxodiferric Intermediate during the Ferroxidase Reaction in Fast Ferritin Mineralization†

Alice S. Pereira,‡ William Small,§ Carsten Krebs,‡ Pedro Tavares,‡ Dale E. Edmondson,*,|| Elizabeth C. Theil,*,§ and Boi Hanh Huynh*,‡

Departments of Physics, Biochemistry, and Chemistry, Rollins Research Building, Emory University, Atlanta, Georgia 30322, and Department of Biochemistry, North Carolina State University, Raleigh, North Carolina 27695

Received April 15, 1998; Revised Manuscript Received May 27, 1998

ABSTRACT: Rapid freeze-quench (RFQ) Mössbauer and stopped-flow absorption spectroscopy were used to monitor the ferritin ferroxidase reaction using recombinant (apo) frog M ferritin; the initial transient ferric species could be trapped by the RFQ method using low iron loading (36 Fe^{2+}/ferritin molecule). Biphasic kinetics of ferroxidation were observed and measured directly by the Mössbauer method; a majority (85%) of the ferrous ions was oxidized at a fast rate of $\sim$80 s^{-1} and the remainder at a much slower rate of $\sim$1.7 s^{-1}. In parallel with the fast phase oxidation of the Fe^{2+} ions, a single transient iron species is formed which exhibits magnetic properties (diamagnetic ground state) and Mössbauer parameters ($\Delta E_Q = 1.08 \pm 0.03$ mm/s and $\delta = 0.62 \pm 0.02$ mm/s) indicative of an antiferromagnetically coupled peroxodiferric complex. The formation and decay rates of this transient diiron species measured by the RFQ Mössbauer method match those of a transient blue species ($\lambda_{max} = 650$ nm) determined by the stopped-flow absorbance measurement. Thus, the transient colored species is assigned to the same peroxodiferric intermediate. Similar transient colored species have been detected by other investigators in several other fast ferritins (H and M subunit types), such as the human H ferritin and the *Escherichia coli* ferritin, suggesting a similar mechanism for the ferritin ferroxidase step in all fast ferritins. Peroxodiferric complexes are also formed as early intermediates in the reaction of O_2 with the catalytic diiron centers in the hydroxylase component of soluble methane monooxygenase (MMOH) and in the D84E mutant of the R2 subunit of *E. coli* ribonucleotide reductase. The proposal that a single protein site, with a structure homologous to the diiron centers in MMOH and R2, is involved in the ferritin ferroxidation step is confirmed by the observed kinetics, spectroscopic properties, and purity of the initial peroxodiferric species formed in the frog M ferritin.

Iron is an important nutrient, required in almost every aspect of cellular function. However, at physiological pH and under oxidizing conditions, the predominant form of iron is Fe^{3+}, which is highly insoluble. How living organisms sequester and mobilize iron for cellular utilization is therefore a question of fundamental importance. Also, in the presence of O_2, free Fe^{2+} ions are extremely toxic, capable of generating hydrogen peroxide, superoxide, and other reactive oxygen species that can attack and destroy important cellular molecules. Ferritin, the iron storage protein found in many

† This work was supported in part by National Institutes of Health Grants GM 47295 (to B.H.H. and D.E.E.) and DK 20251 (to E.C.T.).

* Corresponding authors.
‡ Department of Physics, Emory University.
§ North Carolina State University.
|| Departments of Biochemistry and Chemistry, Emory University.

S0006-2960(98)00847-2 CCC: $15.00
Published on Web 06/25/1998

living organisms, including bacteria, insects, plants, invertebrates, and vertebrates, is unique in the sense that it performs dual functions of (i) detoxifying iron, by oxidizing the Fe^{2+} ions in solution, and (ii) concentrating iron, by storing the oxidized Fe^{3+} ions in its inner protein cavity in the form of a ferrihydrite ($Fe_2O_3 \cdot nH_2O$) phosphate mineral core (refs *1* and *2* and references therein). It is the only known protein that can bind metal ions in solution and convert them into a solid phase mineral.

The ferritin molecule is comprised of 24 polypeptide chains (subunits) organized into a hollow spherical protein shell with a molecular mass of ~480 kDa with an outer diameter of approximately 120 Å and an inner diameter of about 80 Å (*1*, *2*). Vertebrate ferritin molecules are composed of two types of subunits, H and L. The composition of the H and L subunits in a ferritin molecule varies depending on its source of origin. Ferritins from heart and brain are rich in H subunits, while ferritins from liver and spleen are rich in the L form. A third type of subunit, M, found in amphibians, is very homologous in sequence to the H subunit. The H and M subunits from frog differ by only 19 amino acids. Ferritins from invertebrates, plants, and bacteria have sequences more similar to H subunits than to L subunits. A fourth type of ferritin found in bacteria, called bacterioferritin, has hemes bridging pairs of subunits in the 24-mer molecule (*3*). The bacterium *Escherichia coli* contains both ferritin and bacterioferritin. Despite the differences in their amino acid sequences, all types of ferritin subunits are folded into structurally homologous four-α-helix bundles that assemble into similar molecular structures (*3*−*6*).

Ferritin can be reconstituted in vitro by reacting apoferritin (i.e., iron free) with ferrous ions in the presence of molecular oxygen. This ability of apoferritin to catalyze Fe^{2+} oxidation for the nucleation of the mineral core is known as the ferroxidase activity. Studies using recombinant H homopolymers or L homopolymers suggested that the ferroxidase activity is associated only with the H subunits and not with the L subunits (*7*, *8*). On the basis of a series of kinetic, spectroscopic, and mutagenesis investigations (*7*−*13*), a catalytic site for ferritin ferroxidation has been proposed. This catalytic site is suggested to be a diiron site that is structurally homologous to the carboxylate-bridged diiron centers of certain non-heme oxygen reactive enzymes, such as the R2 subunit of *E. coli* ribonucleotide reductase (*14*, *15*) and the hydroxylase component of the soluble methane monooxygenase (MMOH) (*16*, *17*). Although iron is a substrate in ferritin and a catalyst in MMOH and R2, a variety of observations support the above proposal that similar diiron sites are involved in the ferroxidation step in ferritin and in the oxygen activation reactions of the diiron proteins. For example, the X-ray crystallographic structure determined for a Tb derivative of the recombinant H subunit of human liver ferritin shows a binuclear Tb^{3+} binding site (*9*), similar to the diiron sites of R2 and MMOH. The residues involved in the metal binding are E23, E58 (bridging ligand), H61, E57, and E103[1] (Figure 1). These residues are highly conserved in H-type subunits and, except for E57, are not conserved in L-type subunits. Mutations of these residues substantially decrease the ferroxidase activity (*7*, *8*, *10*, *13*). Also, the E58XXH61 sequence is homologous to the diiron binding sequence motif found in the oxygen-reactive enzymes. However, in H ferritins, this sequence motif appears only once in each subunit, while in R2 and MMOH, it appears twice (*14*−*17*). In this respect, the *E. coli* bacterioferritin is more homologous to the diiron enzymes in that the EXXH motif appears twice in the sequence (*2*). A crystallographic study (*3*) of *E. coli* bacterioferritin indicates that this putative ferroxidase site is capable of binding metal (in this case, the metal is Mn^{2+}) and exhibits a structure that is remarkably similar to the diiron sites of R2. Also, Mössbauer investigations of recombinant human H ferritins (*7*, *10*, *18*−*20*) and *E. coli* bacterioferritin (*21*) reconstituted with low iron loading (12−48 Fe/ferritin molecule) show the presence of Mössbauer components indicative of μ-oxo diferric clusters. Although these observations are intriguing, direct evidence supporting the involvement of a diiron site in the ferroxidase process has not been reported.

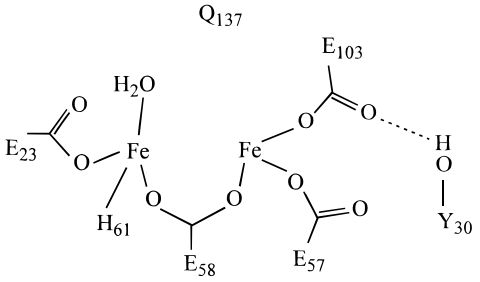

FIGURE 1: Schematic drawing of a proposed structure for the ferroxidase site in human H ferritin.

Recently, a fast-forming purple Fe^{3+}−tyrosinate intermediate with an absorption maximum at 550 nm was found in the reconstitution of recombinant frog H ferritin, providing the first evidence for direct involvement of a specific amino acid residue in the ferroxidase reaction (*22*, *23*). By using the rapid freeze-quench (RFQ) Mössbauer technique, the pseudo-first-order rate for Fe^{2+} oxidation catalyzed by the recombinant H ferritin was determined directly (*24*) and was found to parallel the formation rate of this Fe^{3+}−tyrosinate species, indicating that this protein-bound iron species is among the first products formed immediately after ferroxidation. On the basis of the RFQ Mössbauer measurements, four distinct ferric−oxy multimers (three binuclear iron clusters and one trinuclear iron cluster) are formed in parallel immediately following ferroxidation and subsequently decay to a superparamagnetic "young" mineral core (*24*). The three dimers could be distinguished by their different ΔE_Q values: 0.7, 1.2, and 1.7 mm/s. More recently, a transient blue-colored ($\lambda_{max} = 650$ nm), presumably, Fe^{3+} species was found to form in the reconstitution of recombinant frog M ferritin (*25*). Under the same experimental conditions, the 650 nm species in the M ferritin forms even faster than the 550 nm Fe^{3+}−tyrosinate species in the recombinant frog H ferritin (*22*−*24*). A similar transient blue species with a λ_{max} at 650 nm has also been reported for the recombinant human H ferritin (*13*) and the non-heme *E. coli* ferritin (*26*), and has been proposed (*26*) to be a peroxodiferric intermediate similar to that found in the reaction of O_2 with reduced

[1] The original numbering system introduced for ferritin (*43*) is used in this paper. Another numbering system commonly used in ferritin in the literature differs from the original numbering system by 4. Thus, for example, H61 in this paper is the same as H65 in others (e.g., refs *2* and *9*).

MMOH (*27*). In this paper, we report a RFQ Mössbauer investigation on the ferroxidase reaction catalyzed by recombinant frog M ferritin under the low-iron loading condition. A single transient iron species is formed in parallel with the oxidation of the Fe^{2+} ions with Mössbauer parameters suggestive of a peroxodiferric compound. This result provides the first direct spectroscopic evidence for the involvement of a diiron site in ferritin ferroxidase activity. Since a peroxodiferric species has also been found as the first reaction intermediate formed in the reaction of O_2 with MMOH (*27*) and with the D84E-R2 mutant (*28*), observation of a peroxodiferric species in the initial stage of M ferritin mineralization strongly suggests a similar mechanism for ferritin ferroxidation and for oxygen activation reaction by diiron proteins. However, the diferric peroxo intermediates detected in ferritin and in the diiron proteins exhibit differing Mössbauer parameters, and both the role and the fate of the iron oxidized in ferritin differ from those in MMOH and R2.

METHODS

Protein Purification. The frog M ferritin protein was purified from clone 1D10, subcloned in a Pet 3a vector as previously described for frog recombinant proteins (*22*, *24*, *25*). Betaine and sorbital were always omitted from the culture medium for the M subunit ferritin to increase yields, but betaine (1 mM) was present in the sonication and purification buffers as before (*6*, *22*, *24*, *25*). Recombinant frog ferritins have very low levels of endogenous iron (two or three Fe atoms/ferritin molecule) which eliminates the need to use thioglycollic acid to remove endogenous iron (~30−100 Fe/ferritin molecule) in other studies (*4*, *9*, *10*).

Mössbauer and Stopped-Flow Absorbance Measurements. RFQ Mössbauer samples were prepared as described previously (*24*) using an Update Instruments rapid freeze-quench apparatus. Mössbauer spectra were recorded in either a weak-field spectrometer equipped with a Janis 8DT variable-temperature cryostat or a strong-field spectrometer furnished with a Janis CNDT/SC SuperVaritemp cryostat encasing an 8 T superconducting magnet. Both spectrometers operate in a constant acceleration mode in a transmission geometry. The zero velocity of the spectra refers to the centroid of a room-temperature spectrum of a metallic iron foil. Stopped-flow absorbance measurements were taken using an apparatus purchased from Kinetic Instruments (Ann Arbor, MI). Time-dependent absorbance kinetic traces were collected using a Nicolet 4094 digital oscilloscope. The digital kinetic data were transferred to a personal computer for further analysis. Apoferritin solutions, in 0.2 M MOPS buffer (pH 7) and 0.2 M NaCl, were oxygenated to saturation under 1 atm of O_2 and then mixed with O_2-saturated acidic $FeSO_4$ solutions in 0.2 M NaCl at 23 °C. For the preparation of the Mössbauer samples, an ^{57}Fe-enriched (≥95% enrichment) $FeSO_4$ solution was made from an enriched iron metal foil (*24*). The final protein concentration after mixing was 49 μM (of 24-mer ferritin molecules) for the Mössbauer samples and 25 μM for the stopped-flow measurements. The Fe:ferritin molecule ratio was kept at 36 for both experiments.

RESULTS

To increase the chance of observing the initial oxidizing iron species and to compare the results with those obtained in our earlier investigation on the ferroxidase reaction of recombinant frog H ferritin (*24*), the same small Fe loading (36 Fe^{2+}/ferritin molecule) was used in this study of recombinant frog M ferritin. The rapid freeze-quench method was used to quench the reaction of apoferritin with Fe^{2+} in the presence of O_2 at 25 ms, 60 ms, 130 ms, 220 ms, 440 ms, and 1 s. The decay of the Fe^{2+} ions as a function of time was measured directly by Mössbauer spectroscopy using the method described previously (*24*). The results are shown in Figure 2A. Similar to that for frog H ferritin (*24*), the oxidation of the Fe^{2+} ions catalyzed by frog M ferritin was found to be biphasic. In other words, the data cannot be explained with a single-exponential decay. At least two exponential decay processes are required, and the data are therefore analyzed by using eq 1.

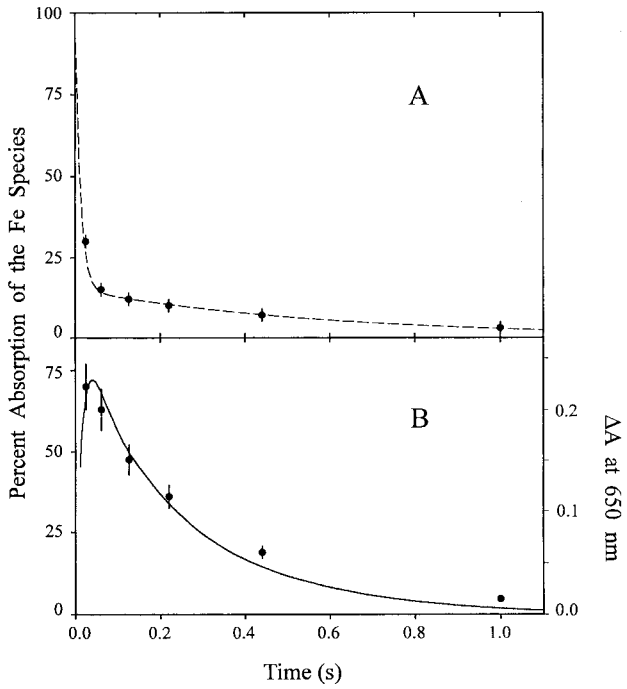

FIGURE 2: Time-dependent behavior of the Fe^{2+} ion (A) and the peroxodiferric intermediate (B) in the early reaction of recombinant frog M apoferritin with Fe^{2+} and O_2 (36 Fe/ferritin molecule). The left ordinate indicates the Mössbauer resonance absorption of the iron species with respect to the absorption of the total iron in the sample (100% absorption represents 36 Fe/ferritin molecule, since the reconstitution was carried out with this Fe:protein ratio). (A) The disappearance of the Fe^{2+} ion. The Mössbauer data are represented by filled circles. The dashed line is the theoretical calculation of eq 2 using the parameters quoted in the text. (B) The formation and decay of the peroxodiferric intermediate. The filled circles are the Mössbauer data, and the vertical bars are the estimated uncertainties. The solid line is the stopped-flow data representing the changes in absorbance at 650 nm as a function of the reaction time.

$$[Fe^{2+}](t) = C_f \exp(-k_f t) + C_s \exp(-k_s t) \qquad (1)$$

Approximately 85% of the Fe^{2+} ions (C_f) oxidized at a fast rate of ~80 s^{-1} (k_f) and 15% of the Fe^{2+} ions (C_s) oxidized at a slower rate of ~1.7 s^{-1} (k_s). The rate of fast Fe^{2+} oxidation by frog M ferritin is much faster than that (~25 s^{-1}) of the H ferritin (*24*), a phenomenon that is also observed by stopped-flow optical measurements (*25*).

As in the case of frog H ferritin, multiple diferric−oxy clusters are also formed in frog M ferritin following the

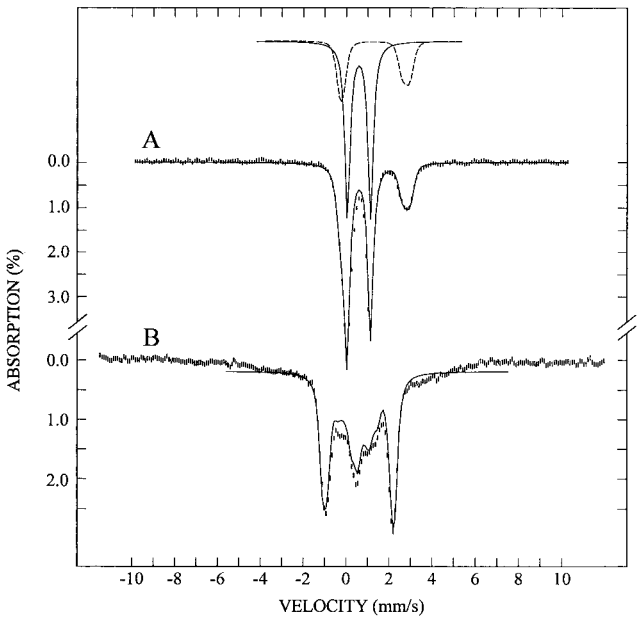

FIGURE 3: Mössbauer spectra of a rapid freeze-quench sample from the reaction of recombinant frog M apoferritin with Fe^{2+} and O_2. The reaction was quenched at 25 ms. The data were recorded at 4.2 K with a magnetic field of 50 mT (A) and 8 T (B) applied parallel to the γ beam. Spectrum A can be analyzed as a superposition of two components. One component (dashed line above the data) with parameters ($\Delta E_Q = 3.00$ mm/s and $\delta = 1.31$ mm/s) typical of high-spin ferrous ions accounts for ~31% of the total iron absorption and represents the not-yet-reacted Fe^{2+} ions. The other component (solid line above the data) accounts for ~69% of the total Fe absorption and is assigned to the peroxodiferric intermediate. The solid line plotted over the data in part A is the superposition of these two components. The solid line in part B is a theoretical simulation of the diferric−peroxo intermediate using the ΔE_Q and δ values obtained from part A with an asymmetry parameter η of 1.3 and assuming diamagnetism.

oxidation of the Fe^{2+} ions. However, a major difference is observed; a lag phase is detected for the formation of these diferric−oxy clusters in M ferritin (unpublished data). During the lag, a novel Fe species, designated as a peroxodiferric species (see below), forms immediately following the fast phase of the ferrous oxidation and subsequently decays coincident with the formation of the diferric−oxy clusters. The transient nature of this novel species is shown in Figure 2B, which reveals that the fast formation of the peroxodiferric species is followed by a slower decay process. The data can therefore be analyzed by eq 2 assuming two irreversible sequential first-order processes with an initial Fe absorption percentage (A_0) of ~85% (i.e., same as C_f), a formation rate k_1 of ~80 s^{-1} (i.e., same as the fast rate of ferrous oxidation), and a decay rate k_2 of about 3−4 s^{-1}.

$$[\text{diferric peroxide}](t) = \frac{A_0 k_1}{k_2 - k_1}[\exp(-k_1 t) - \exp(-k_2 t)] \quad (2)$$

At 25 ms, this species accumulates to a level of 70% of the total iron present in the sample and exhibits a single sharp (line width = 0.3 mm/s) quadrupole doublet in the Mössbauer spectrum recorded at 4.2 K with a weak applied field (Figure 3A). Spectra recorded in a strong field, for example, 8 T (Figure 3B), indicate that this novel species is diamagnetic. The Mössbauer parameters (quadrupole splitting, ΔE_Q = 1.08 ± 0.03 mm/s, and isomer shift δ = 0.62 ± 0.02 mm/s) are characteristic of high-spin ferric. The observed diamagnetism for this new species therefore suggests an antiferromagnetically coupled diferric system. The δ value of 0.62 mm/s is similar to those observed for the peroxodiferric intermediate found in MMOH (0.66 mm/s) (*27*, *29*) and in the D84E mutant of R2 (0.63 mm/s) (*28*). On the basis of these observations and the fact that it forms immediately after apoferritin is reacted with Fe^{2+} and O_2 and subsequently decays to the diferric−oxy clusters, this novel species is proposed to be a diferric−peroxo species similar to those found in the carboxylate-bridged diiron enzymes. However, it should be noted that the ΔE_Q value for this proposed peroxodiferric intermediate in ferritin is smaller than those observed for the diiron enzymes (see Table 1).

Table 1: Spectroscopic Parameters for Peroxodiferric Intermediates in Various Proteins and the Peroxodiferric Model Complex $[Fe_2(\mu\text{-}O_2)(\mu\text{-}O_2CCH_2Ph)_2\{HB(pz')_3\}_2]$

		M ferritin[a]	MMOH[b]	D84E-R2[c]	model complex[d]
optical	λ_{max} (nm)	650	~725	~700	694
	ϵ (cm^{-1} M^{-1})	~1000	~1500	~1500	2650
Mössbauer	ΔE_Q (mm/s)	1.08	1.51	1.58	1.40
	δ (mm/s)	0.62	0.66	0.63	0.66

[a] This work and ref *25*. [b] See refs *27* and *29*. The optical parameters are from the work of A. M. Valentine and S. J. Lippard (unpublished data). [c] See ref *28*. [d] See ref *33*.

To determine whether this novel iron intermediate observed in the Mössbauer measurements is the same intermediate as the transient blue-colored species (λ_{max} = 650 nm) detected optically, stopped-flow kinetic measurements were performed under comparable experimental conditions (see Methods). The change in absorbance at 650 nm as a function of reaction time is plotted in Figure 2B. The agreement between the Mössbauer and optical data is striking. The stopped-flow data can also be analyzed by eq 2 with an initial absorbance (A_0) of 0.27 (normalized for a path length of 1 cm), a formation rate (k_1) of 80 ± 10 s^{-1}, and a decay rate (k_2) of 4.2 ± 0.5 s^{-1}. On the basis of the Mössbauer data (which provide the information on the number of peroxodiferric intermediates formed as a function of time) and the stopped-flow data (which provide the corresponding information on the absorbance at 650 nm), the molar extinction coefficient for this peroxide intermediate is estimated to be approximately 1000 M^{-1} cm^{-1}. Peroxodiferric model complexes exhibit peroxo-to-Fe charge-transfer transitions in the λ_{max} region of 470−700 nm with extinction coefficients ranging from 190 to 3500 M^{-1} cm^{-1} (*30*−*33*).

DISCUSSION

The observation that only one single diiron species formed immediately after Fe^{2+} oxidation provides direct spectroscopic evidence supporting the hypothesis that a single protein site (per subunit) is involved in ferritin ferroxidase reaction and that the site is a diiron site. As mentioned in the introductory section, on the basis of a series of kinetic, spectroscopic, and mutagenesis investigations, it has been proposed that a carboxylate-bridged diiron center, similar to those found in the oxygen-reactive diiron enzymes, is

Scheme 1

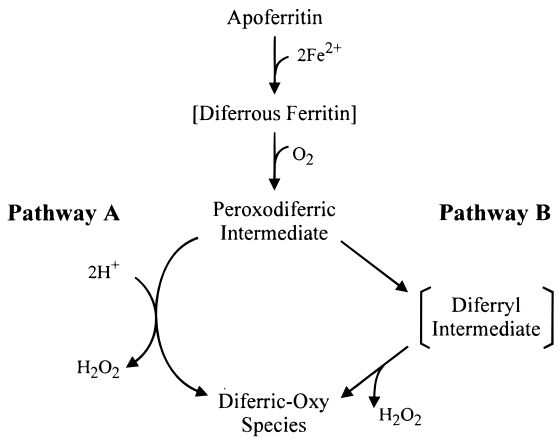

involved in the ferritin ferroxidase reaction (*7*−*13*). The results presented here for the frog M ferritin support such a proposal. Stopped-flow measurements on recombinant human H ferritin (*13*) and *E. coli* ferritin (*26*) also show a transient blue species with a λ_{max} of 650 nm. Consequently, it is very likely that a common ferroxidase mechanism is employed by ferritins with fast rates of iron uptake (i.e., the H- and M-type ferritins). The fact that a peroxodiferric intermediate was not observed in the recombinant frog H ferritin[2] (*24*) does not necessarily indicate a different mechanism. But rather, the kinetic behavior of the peroxo intermediate may be altered in the recombinant frog H ferritin such that the peroxodiferric intermediate does not accumulate to a detectable level. This suggestion is supported by the observation that in the recombinant frog H ferritin the rate of Fe^{2+} oxidation, which should also be the formation rate of the peroxo species, is slower in comparison with those of the frog M ferritin and human H ferritin. Furthermore, all the fast-forming Fe^{3+}−oxy dimers detected in frog H ferritin are also present in frog M ferritin. However, in the case of the M ferritin, all the Fe^{3+}−oxy multimers are dimers; the trimer observed in H ferritin (*24*) is not observed. In addition to the dimers with Mössbauer quadrupole splittings of 0.7, 1.2, and 1.7 mm/s observed in the frog H ferritin (*24*), a new dimer with a quadrupole splitting of ∼2.0 mm/s is seen in the M ferritin (unpublished data). Although formation of a dimer is expected since a diferric peroxide is presumably the precursor, formation of multiple dimers is unusual and probably reflects a flexible ferroxidase site. We, as well as many others, believe that flexibility may be an important factor for ferritin function (*5*, *13*, *22*, *24*). Multiple species with different quadrupole splittings have been observed for the diferric center in the stearoyl-ACP Δ^9 desaturase (*34*).

When the previously reported structural, spectroscopic, and mechanistic investigations (*3*, *4*, *7*−*13*, *18*−*26*, *35*, *36*) are combined with the rapid freeze-quench Mössbauer results obtained for the frog H (*24*) and M (Figures 2 and 3) ferritins, it is possible to propose the following scheme as a working hypothesis for ferritin ferroxidase reaction (Scheme 1). In this hypothetical scheme, the reaction of apoferritin with Fe^{2+} ions begins with binding of two Fe^{2+} ions at the putative ferroxidase site, followed immediately by the reaction of O_2 with the diferrous center forming a peroxodiferric intermediate which exhibits the broad optical absorption at λ_{max} = 650 nm and the sharp Mössbauer quadrupole doublet with a ΔE_Q of 1.08 mm/s and a δ of 0.62 mm/s. The fact that a sharp quadrupole doublet is observed for this diiron intermediate suggests a symmetric binding for the peroxide. The next steps (pathway A) may involve the protonation of the coordinated peroxide ligand and subsequent release of H_2O_2, which has been observed as the primary product of the ferroxidase reaction (*22*, *35*, *36*). Alternatively, the reaction may follow pathway B which suggests the conversion of the diferric−peroxo intermediate to a diferryl complex similar to compound ***Q*** found in the reaction of MMOH with O_2 (*27*, *29*, *37*, *38*). Reaction of this diferryl complex with water molecule(s) may result in the formation of the multiple diferric−oxy clusters (*24*) and release of H_2O_2 (*22*, *35*, *36*). The antiferromagnetic coupling observed for the diferric−oxy clusters indicates the presence of bridging ligands, most probably derived from the O_2 or solvent molecules. The different ΔE_Q values (0.7, 1.2, 1.7, and 2.0 mm/s) may reflect different ligand environments and/or bridging configurations (*39*, *40*); in general, diferric complexes with oxo bridge(s) have larger ΔE_Q values while those with bridging hydroxides have smaller ΔE_Q values (*39*, *40*). Protonation of a bridging hydroxo group to form yet another configuration as proposed for the diferric MMOH (*41*) may also be possible. This latter proposed pathway is consistent with the current available data and is similar to a unifying scheme proposed for the oxygen activation mechanism for MMOH and R2 (*42*). The challenge for future investigations is not only to use the common features of these diiron proteins to understand the iron−dioxygen interaction but also to deconvolute the common properties of each protein from those required for the specific reactions.

[2] It was discovered after our initial investigation that the recombinant frog H ferritin contains a spontaneous mutation L134P; unfortunately, it has been difficult to produce large amounts of the parent frog H ferritin. The mechanistic implications on ferritin ferroxidation of the mutation at L134, a nonliganding residue conserved in both fast and slow ferritins, are not clear at this time.

ACKNOWLEDGMENT

The authors thank Ms. A. M. Valentine and Dr. S. J. Lippard for allowing us to quote their unpublished data for the peroxo intermediate in MMOH.

REFERENCES

1. Waldo, G. S., and Theil, E. C. (1996) in *Comprehensive Supramolecular Chemistry* (Suslick, K. S., Ed.) Vol. 5, pp 65−89, Pergamon Press, Oxford, U.K.
2. Harrison, P. M., and Arosio, P. (1996) *Biochim. Biophys. Acta 1275*, 161−203.
3. Frolow, F., Kalb(Gilboa), A. J., and Yariv, J. (1994) *Struct. Biol. 1*, 453−460.
4. Hempstead, P. D., Yewdall, S. J., Fernie, A. R., Lawson, D. L., Artymiuk, P. J., Rice, D. W., Ford, G. C., and Harrison, P. M. (1997) *J. Mol. Biol. 268*, 424−448.
5. Trikha, J., Theil, E. C., and Allewell, N. M. (1995) *J. Mol. Biol. 248*, 949−967.
6. Trihka, J., Waldo, G. S., Lewandowski, F. A., Theil, E. C., Weber, P. C., and Allewell, N. M. (1994) *Proteins 18*, 107−118.
7. Bauminger, E. R., Harrison, P. M., Hechel, D., Nowik, I., and Treffry, A. (1991) *Biochim. Biophys. Acta 1118*, 48−58.
8. Sun, S., Arosio, P., Levi, S., and Chasteen, N. D. (1993) *Biochemistry 32*, 9362−9369.

9. Lawson, D. M., Artymiuk, P. J., Yewdall, S. J., Smith, J. M. A., Livingstone, J. C., Treffry, A., Luzzago, A., Levi, S., Arosio, P., Cesareni, G., Thomas, C. D., Shaw, W. V., and Harrison, P. M. (1991) *Nature 349*, 541−544.
10. Bauminger, E. R., Harrison, P. M., Hechel, D., Hodson, N. W., Nowik, I., Treffry, A., and Yewdall, S. J. (1993) *Biochem. J. 196*, 709−719.
11. Hempstead, P. D., Hudson, A. J., Artymiuk, P. J., Andrews, S. C., Banfield, M. J., Guest, J. R., and Harrison, P. M. (1994) *FEBS Lett. 350*, 258−262.
12. Treffry, A., Zhao, Z., Quail, M. A., Guest, J. R., and Harrison, P. M. (1997) *Biochemistry 36*, 432−441.
13. Treffry, A., Zhao, Z., Quail, M. A., Guest, J. R., and Harrison, P. M. (1995) *Biochemistry 34*, 15204−15213.
14. Nordlund, P., Sjöberg, B.-M., and Eklund, H. (1990) *Nature 345*, 593−598.
15. Logan, D. T., Su, X.-D., Åberg, A., Regnströrn, K., Hajdu, J., Eklund, H., and Nordlund, P. (1996) *Structure 4*, 1053−1064.
16. Rosenzweig, A. C., Nordlund, P., Takahara, P. M., Frederick, C. A., and Lippard, S. J. (1995) *Chem. Biol. 2*, 409−418.
17. Elango, N., Radhakrishnan, R., Froland, W. A., Wallar, B. J., Earhart, C. A., Lipscomb, J. D., and Ohlendorf, D. H. (1997) *Protein Sci. 6*, 556−568.
18. Bauminger, E. R., Harrison, P. M., Nowik, I., and Treffry, A. (1989) *Biochemistry 28*, 5486−5493.
19. Treffry, A., Bauminger, E. R., Hechel, D., Hodson, N. W., Nowik, I., Yewdall, S. J., and Harrison, P. M. (1993) *Biochem. J. 296*, 721−728.
20. Bauminger, E. R., Treffry, A., Hudson, A. J., Hechel, D., Hodson, N. W., Andrews, S. C., Levi, S., Nowik, I., Arosio, P., Guest, J. R., and Harrison, P. M. (1994) *Biochem. J. 302*, 813−820.
21. Hawkins, C., Treffry, A., Mackey, J. B., Williams, J. M., Andrews, S. C., Guest, J. R., and Harrison, P. M. (1996) *Nuovo Cimento D 18*, 347−352.
22. Waldo, G. S., and Theil, E. C. (1993) *Biochemistry 32*, 13262−13269.
23. Waldo, G. S., Ling, J., Sanders-Loehr, J., and Theil, E. C. (1993) *Science 259*, 796−798.
24. Pereira, A. S., Tavares, P., Lloyd, S. G., Danger, D., Edmondson, D. E., Theil, E. C., and Huynh, B. H. (1997) *Biochemistry 36*, 7917−7927.
25. Fetter, J., Cohen, J., Danger, D., Sanders-Loehr, J., and Theil, E. C. (1997) *J. Biol. Inorg. Chem. 2*, 652−661.
26. Zhao, Z., Treffry, A., Quail, M. A., Guest, J. R., and Harrison, P. M. (1997) *J. Chem. Soc., Dalton Trans*., 3977−3978.
27. Liu, K. E., Wang, D., Huynh, B. H., Edmondson, D. E., Salifoglou, A., and Lippard, S. J. (1994) *J. Am. Chem. Soc. 116*, 7465−7466.
28. Bollinger, J. M., Jr., Krebs, C., Vicol, A., Chen, S., Ley, B. A., Edmondson, D. E., and Huynh, B. H. (1998) *J. Am. Chem. Soc. 120*, 1094−1095.
29. Liu, K., Valentine, A. M., Wang, D., Huynh, B. H., Edmondson, D. E., Salifoglou, A., and Lippard, S. J. (1995) *J. Am. Chem. Soc. 117*, 10174−10185.
30. Que, L., Jr., and True, A. E. (1990) *Prog. Inorg. Chem. 38*, 97−200.
31. Menage, S., Brennan, B. A., Juarez-Garcia, C., Münck, E., and Que, L., Jr. (1990) *J. Am. Chem. Soc. 112*, 6423−6425.
32. Kitajima, N., Tamura, N., Amagai, H., Fukui, H., Moro-oka, Y., Mizutani, Y., Kitagawa, T., Mathur, R., Heerwegh, K., Reed, C. A., Randall, C. R., Que, L., Jr., and Tatsumi, K. (1994) *J. Am. Chem. Soc. 116*, 9071−9085.
33. Kim, K., and Lippard, S. J. (1996) *J. Am. Chem. Soc. 118*, 4914−4915.
34. Fox, G. B., Shanklin, J., Somerville, C., and Münck, E. (1993) *Proc. Natl. Acad. Sci. U.S.A. 90*, 2486−2490.
35. Xu, L. B., and Chasteen, N. D. (1991) *J. Biol. Chem. 266*, 19965−19970.
36. Sun, S., Arosio, P., Levi, S., and Chasteen, N. D. (1993) *Biochemistry 32*, 9362−9369.
37. Lee, S.-K., Fox, B. G., Froland, W. A., Lipscomb, J. D., and Münck, E. (1993) *J. Am. Chem. Soc. 115*, 6450−6451.
38. Lee, S.-K., Nesheim, J. C., and Lipscomb, J. D. (1993) *J. Biol. Chem. 268*, 21569−21577.
39. Hartman, J. R., Rardin, R. L., Chaudhuri, P., Pohl, K., Wieghardt, K., Nuber, B., Weiss, J., Papaefthymiou, G., Frankel, R. B., and Lippard, S. J. (1987) *J. Am. Chem. Soc. 109*, 7387−7396.
40. Kurtz, D. M., Jr. (1990) *Chem. Rev. 90*, 585−606.
41. Shu, L., Liu, Y., Lipscomb, J. D., and Que, L., Jr. (1996) *J. Biol. Inorg. Chem. 1*, 297−304.
42. Edmondson, D. E., and Huynh, B. H. (1996) *Inorg. Chim. Acta 252*, 399−404.
43. Rice, D. W., Ford, G. C., White, J. L., Smith, J. M. A., and Harrison, P. M. (1983) *Adv. Inorg. Biochem. 5*, 39−50.

BI980847W